Article

External Electric Field Effects on State Energy and Photoexcitation Dynamics of Diphenylpolyenes

Takakazu Nakabayashi, Md. Wahadoszamen, and Nobuhiro Ohta

J. Am. Chem. Soc., **2005**, 127 (19), 7041-7052• DOI: 10.1021/ja0401444 • Publication Date (Web): 21 April 2005

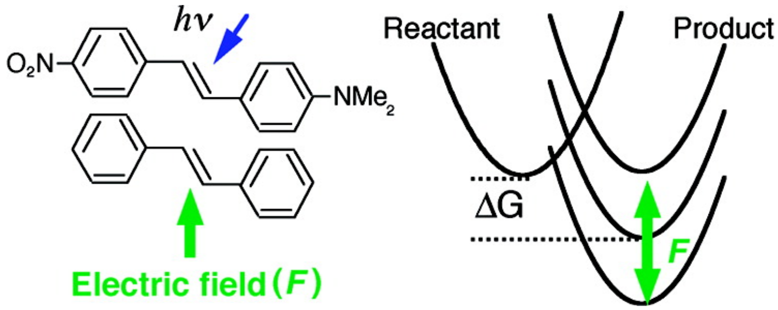

Journal of the American Chemical Society is published by the American Chemical Society. 1155 Sixteenth Street N.W., Washington, DC 20036

J|A|C|S
ARTICLES

External Electric Field Effects on State Energy and Photoexcitation Dynamics of Diphenylpolyenes

Takakazu Nakabayashi,*,†,‡ Md. Wahadoszamen,‡ and Nobuhiro Ohta*,†,‡

Contribution from the Research Institute for Electronic Science (RIES), Hokkaido University, Sapporo, 060-0812, Japan, and Graduate School of Environmental Earth Science, Hokkaido University, Sapporo, 060-0810, Japan

Received May 24, 2004; E-mail: takan@es.hokudai.ac.jp; nohta@es.hokudai.ac.jp

---

Abstract: External electric field effects on state energy and photoexcitation dynamics have been examined for *para*-substituted and unsubstituted all-*trans*-diphenylpolyenes doped in a film, based on the steady-state and picosecond time-resolved measurements of the field effects on absorption and fluorescence. The substitution dependence of the electroabsorption spectra shows that the dipole moment of the substituted stilbene in the Franck−Condon excited state becomes larger with increasing difference between the Hammet constants of the substituents. Fluorescence quantum yields of 4-(dimethylamino)-4′-nitrostilbene and 4-(dimethylamino)-4′-nitrodiphenylbutadiene are markedly reduced by an electric field, suggesting that the rates of the intramolecular charge transfer (CT) from the fluorescent state to the nonradiative CT state are accelerated by an external electric field. The magnitude of the field-induced decrease in fluorescence lifetime has been evaluated. The isomerization of the unsubstituted all-*trans*-diphenylpolyenes to the *cis* forms is shown to be a significant nonradiative pathway even in a film. Field-induced quenching of their fluorescence as well as field-induced decrease in fluorescence lifetime suggests that the *trans* to *cis* photoisomerization is enhanced by an electric field.

---

1. Introduction

The optical properties of polyenes have been the subject of wide investigation over the past two decades. Polyene derivatives such as carotenoid and retinoid series play crucial roles in many biological photoactive systems including photosensory and photoenergy transductions.[1−5] The *cis*−*trans* photoisomerization of olefins, which is one of the most fundamental chemical reactions, has been studied as a model for barrier-crossing reactions.[6−11] Further, the radical ions and divalent ions of polyenes are useful for an understanding of the structures and dynamics of self-localized excitations in conducting polymers,[12] and polyenes with electron-donating and -accepting substituents are promising nonlinear photonic materials because of their high second- and third-order polarizabilities.[13,14] Donor−acceptor-substituted polyenes also show laser gain properties[15] and serve as model systems for intramolecular charge transfer (ICT).[16]

External electric field effects on optical spectra have been extensively applied in molecular spectroscopy to examine the electronic structures in excited states. The so-called electroabsorption and electrofluorescence spectra (plots of the electric-field-induced change in absorption intensity and fluorescence intensity as a function of wavelength, respectively) are extremely useful to understand the mechanism of molecular dynamics following photoexcitation.[17,18] These spectra are especially powerful for studying CT dynamics because of its high sensitivity to an electric field.[17−21] Application of external electric fields may also give a new way to control photochemical reactions.

In the present paper, we report the electroabsorption and electrofluorescence spectra of *para*-substituted and unsubstituted all-*trans*-diphenylpolyenes in a poly(methyl methacrylate) (PMMA) film. The electronic structures in excited states and the mechanisms of the ICT and photoisomerization dynamics are discussed on the basis of the results obtained. The *trans*

[†] Research Institute for Electronic Science.

[‡] Graduate School of Environmental Earth Science.

(1) Koyama, Y.; Kuki, M.; Andersson, P. O.; Gillbro, T. *Photochem. Photobiol.* **1996**, *63*, 243.
(2) Birge, R. R. *Biochim. Biophys. Acta* **1990**, *1016*, 293.
(3) Khorana, H. G. *J. Biol. Chem.* **1992**, *267*, 1.
(4) Spudich, E. N.; Zhang, W.; Alam, M.; Spudich, J. L. *Proc. Natl. Acad. Sci. U.S.A.* **1997**, *94*, 4960.
(5) Luecke, H. *Biochim. Biophys. Acta* **2000**, *1460*, 133.
(6) Courtney, S. H.; Fleming, G. R. *J. Chem. Phys.* **1985**, *83*, 215.
(7) Allen, M. T.; Whitten, D. G. *Chem. Rev.* **1989**, *89*, 1691.
(8) Saltiel, J.; Sun, Y.-P. In *Photochromism, Molecules and Systems*; Dürr, H., Bouas-Laurent, H., Eds.; Elsevier: Amsterdam, 1990; pp 64−164.
(9) Waldeck, D. H. *Chem. Rev.* **1991**, *91*, 415.
(10) Görner, H.; Kuhn, H. J. *Adv. Photochem.* **1995**, *19*, 1.
(11) Hamaguchi, H.; Iwata, K. *Bull. Chem. Soc. Jpn.* **2002**, *75*, 883.
(12) Furukawa, Y. *J. Phys. Chem.* **1996**, *100*, 15644.
(13) Kanis, D. R.; Ratner, M. A.; Marks, T. J. *Chem. Rev.* **1994**, *94*, 195.
(14) Beljonne, D.; Brédas, J.-L.; Cha, M.; Torruellas, W. E.; Stegeman, G. I.; Hofstraat, J. W.; Horsthuis, W. H. G.; Möhlmann, G. R. *J. Chem. Phys.* **1995**, *103*, 7834.
(15) Kobayashi, T.; Terauchi, M.; Uchiki, H. *Chem. Phys. Lett.* **1986**, *126*, 143.
(16) Rettig, W.; Majenz, W.; Lapouyade, R.; Haucke, G. *J. Photochem. Photobiol. A: Chem.* **1992**, *62*, 415.
(17) Bublitz, G. U.; Boxer, S. G. *Annu. Rev. Phys. Chem.* **1997**, *48*, 213.
(18) Ohta, N. *Bull. Chem. Soc. Jpn.* **2002**, *75*, 1637.
(19) Ohta, N.; Koizumi, M.; Umeuchi, S.; Nishimura, Y.; Yamazaki, I. *J. Phys. Chem.* **1996**, *100*, 16466.
(20) Ohta, N.; Umeuchi, S.; Nishimura, Y.; Yamazaki, I. *J. Phys. Chem. B* **1998**, *102*, 3784.
(21) Wahadoszamen, Md.; Nakabayashi, T.; Ohta. N. *Chem. Phys. Lett.* **2004**, *387*, 124.

10.1021/ja0401444 CCC: $30.25 © 2005 American Chemical Society

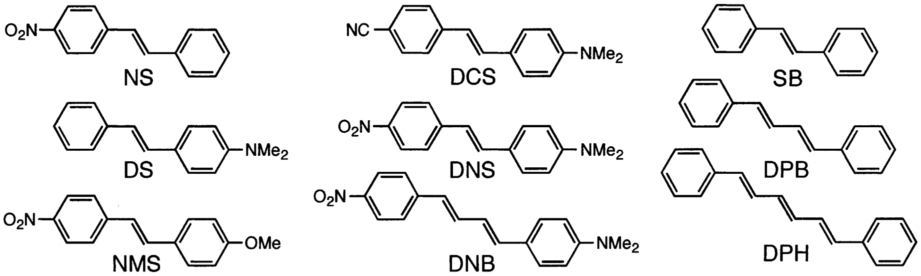

Figure 1. Chemical structures of diphenylpolyenes treated in the present study.

isomers of 4-nitrostilbene (NS), 4-dimethylaminostilbene (DS), 4-(nitro)-4′-methoxystilbene(NMS),4-(dimethylamino)-4′-cyanostilbene (DCS), 4-(dimethylamino)-4′-nitrostilbene (DNS), and all-*trans*-4-(dimethylamino)-4′-nitrodiphenylbutadiene (DNB) have been used as a series of substituted diphenylpolyenes. We have also used *trans*-stilbene (SB), all-*trans*-diphenylbutadiene (DPB), and all-*trans*-diphenylhexatriene (DPH) as a series of unsubstituted diphenylpolyenes. The chemical structures of the diphenylpolyenes used in the present study are shown in Figure 1.

There have been a large number of studies on the photophysical properties of donor−acceptor-substituted stilbenes.[22−43] Among them, DNS, one of the donor−acceptor-substituted stilbenes, is expected to have a very high optical nonlinear susceptibility because of its large permanent dipole moments especially in excited singlet states.[13,14] This molecule also shows a characteristic solvent dependence in photophysical behavior, which is ascribed to the formation of a CT state upon photoexcitation.[22−36] If the empirical Dimroth parameter $E_T(30)$ is used as a measure of solvent polarity,[44] the quantum yields both of the *trans*−*cis* photoisomerization and of the intersystem crossing decrease with increasing $E_T(30)$ value (i.e., increasing solvent polarity). In solvents with the $E_T(30)$ values larger than ~36 kcal mol^{-1} (dioxane, for example), the yields of these processes are nearly zero. On the other hand, the fluorescence quantum yield increases as the $E_T(30)$ value increases in the region below ~33−34 kcal mol^{-1} (toluene, for example) and drastically decreases with the increase of the $E_T(30)$ value above ~36 kcal mol^{-1} to become almost null in acetonitrile ($E_T(30) = 46.0$ for acetonitrile). To account for such a strong decrease of the fluorescence yield in polar solvents (~0.53 in toluene and <0.002 in acetonitrile), a rapid transition from the lowest optically allowed excited state (locally excited state, LE state) to a “nonradiative” intermediate state has been suggested in polar solvents. From the preferential generation in highly polar solvents, this intermediate state has been considered to be a CT state having a much larger dipole moment than the LE state. This CT state relaxes nonradiatively to the electronically ground (S_0) state. It has been proposed that the nonradiative CT species has a structure with the NO_2 group twisted from the plane of the benzene ring.[28,29] Several groups have measured transient vibrational spectra of DNS in polar solvents.[30,31,35] The position of the NO_2 symmetric stretching band of the CT species was found to exhibit a marked dependence on the solvent.[30] It has been suggested that DNB, which has a conjugated hydrocarbon chain longer than DNS, also gives a nonradiative CT state in polar solvents.[27,37] On other donor−acceptor-substituted stilbenes, characteristics of electronically excited CT states have also been discussed.[38−43]

The photochemistry of SB following UV excitation has been studied as a prototype of *cis*−*trans* photoisomerization.[6−11] This photoisomerization is known to take place on the potential energy surface of the lowest excited singlet (S_1) state and result in the formation of the *cis* isomer with a quantum yield of about 0.5 in solution.[45,46] A great number of studies have been devoted to clarify this process; however, the detailed mechanism of the *cis*−*trans* photoisomerization has not yet been understood, which may arise from the ambiguity of the geometrical and electronic structures of SB around the conical intersection region. In the present paper, we discuss the electronic structures of the unsubstituted diphenylpolyenes in the S_1 state around the conical intersection region using electric field modulation spectroscopy. Investigation of electric field effects on photoisomerization is also important from a biological point of view, since protein membranes surrounding chromophores produce strong electric fields in some cases.[47,48]

We focus on electric field effects on the photoexcitation dynamics of DNS, DNB, and SB in the present paper. The contents discussed in the present paper are as follows. We first examine the substitution dependence of the difference in electric dipole moment between the S_0 state and the Franck−Condon excited (FC) state by analyzing the electroabsorption spectra

---

(22) Bent, D. V.; Schulte-Frohlinde, D. *J. Phys. Chem.* **1974**, *78*, 446.
(23) Görner, H.; Schulte-Frohlinde, D. *Ber. Bunsen-Ges. Phys. Chem.* **1978**, *82*, 1102.
(24) Kawski, A.; Ostrowska, B.; Ston, M. *Z. Naturforsch. A* **1981**, *36*, 999.
(25) de Haas. M. P.; Warman, J. M. *Chem. Phys.* **1982**, *73*, 35.
(26) Görner, H. *J. Photochem. Photobiol. A: Chem.* **1987**, *40*, 325.
(27) Shin, D. M.; Whitten, D. G. *J. Phys. Chem.* **1988**, *92*, 2945.
(28) Gruen, H.; Görner, H. *J. Phys. Chem.* **1989**, *93*, 7144.
(29) Lapouyade, R.; Kuhn, A.; Létard, J.-F.; Rettig, W. *Chem. Phys. Lett.* **1993**, *208*, 48.
(30) Nakabayashi, T.; Okamoto, H.; Tasumi, M. *J. Raman Spectrosc.* **1995**, *26*, 841.
(31) Okamoto, H.; Tasumi, M. *Chem. Phys. Lett.* **1996**, *256*, 502.
(32) Gurzadyan, G.; Görner, H. *Chem. Phys. Lett.* **2000**, *319*, 164.
(33) Rijkenberg, R. A.; Bebelaar, D.; Buma, W. J.; Hofstraat, J. W. *J. Phys. Chem. A* **2002**, *106*, 2446.
(34) Moran, A. M.; Bartholomew, G. P.; Bazan, G. C.; Kelley, A. M. *J. Phys. Chem. A* **2002**, *106*, 4928.
(35) Oberlé, J.; Jonusauskas, G.; Abraham, E.; Lapouyade, R.; Rullière, C. *Bull. Chem. Soc. Jpn.* **2002**, *75*, 1041.
(36) Farztdinov, V. M.; Ernsting, N. P. *Chem. Phys.* **2002**, *277*, 257.
(37) Lin, C. T.; Guan, H. W.; McCoy, R. K.; Spangler, C. W. *J. Phys. Chem.* **1989**, *93*, 39.
(38) Görner, H. *J. Photochem. Photobiol.* **1980**, *13*, 269.
(39) Safarzadeh-Amiri, A. *Chem. Phys. Lett.* **1986**, *125*, 272.
(40) Lapouyade, R.; Czeschka, K.; Majenz, W.; Rettig, W.; Gilabert, E.; Rullière, C. *J. Phys. Chem.* **1992**, *96*, 9643.
(41) Il'ichev, Yu. V.; Kühnle, W.; Zachariasse, K. A. *Chem. Phys.* **1996**, *211*, 441.
(42) Létard, J.-F.; Lapouyade, R.; Rettig, W. *J. Am. Chem. Soc.* **1993**, *115*, 2441.
(43) Lewis, F. D.; Weigel, W. *J. Phys. Chem. A* **2000**, *104*, 8146.
(44) Reichardt, C. *Angew. Chem., Int. Ed. Engl.* **1979**, *18*, 98.
(45) Saltiel, J. *J. Am. Chem. Soc.* **1968**, *90*, 6394.
(46) Saltiel, J.; Waller, A. S.; Sears, D. F., Jr. *J. Am. Chem. Soc.* **1993**, *115*, 2453.
(47) Ogrodnik, A.; Eberl, U.; Heckmann, R.; Kappl, M.; Feick, R.; Michel-Beyerle, M. E. *J. Phys. Chem.* **1991**, *95*, 2036.
(48) Kochendoerfer, G. G.; Lin, S. W.; Sakmar, T. P.; Mathies, R. A. *Trends Biochem. Sci.* **1999**, *24*, 300.

of the substituted diphenylpolyenes. Next, we observe the electrofluorescence spectra of the substituted diphenylpolyenes and the field-induced change in fluorescence decay profile for DNS and DNB. Electric field effects on the ICT dynamics are discussed on the basis of the results obtained. Finally, we analyze the electroabsorption and electrofluorescence spectra of the unsubstituted diphenylpolyenes to obtain information on the electronic structures of the intermediates in the photoisomerization.

2. Experimental Section

DNB and DCS were synthesized and purified according to refs 27 and 39, respectively. Commercially available DNS (Eastman Kodak Co.) was recrystallized twice from a benzene−ethanol mixture. The other molecules employed in the present study were purchased from Tokyo Kasei Co. and recrystallized twice from ethanol or ethanol and benzene. A certain amount of benzene solution of PMMA containing diphenylpolyenes was cast on an indium−tin-oxide (ITO) coated quartz substrate by a spin coating method. A semitransparent aluminum (Al) film was deposited on the dried polymer film by a vacuum vapor deposition technique. The ITO and Al films were used as electrodes. The thickness of the film was typically 0.4 μm. The concentration of the sample was in the range 0.05−0.5 mol % in its ratio to the monomer unit of PMMA. In this concentration range, the shape and position of the spectra and their field-induced changes were independent of the concentration within the experimental accuracy, indicating that the interaction between dye chromophores is negligible in the present experimental conditions. Most of the chromophores exist as the monomer species in the present study. In other dye molecules such as pyrene, it has also been known that the observed spectra arise from the monomer species in the concentration region less than 1.0 mol %.[18]

All the measurements were performed at room temperature under vacuum conditions. Electric-field-induced changes in steady-state absorption and fluorescence spectra were measured using electric field modulation spectroscopy with the same apparatus as described elsewhere.[19−21] A modulation in absorption intensity or fluorescence intensity was induced by a sinusoidal ac voltage with a modulation frequency of 40 Hz. Field-induced change in absorption intensity or fluorescence intensity was detected with a lock-in amplifier (Stanford Research Systems, SR830) at the second harmonic of the modulation frequency. A dc component of the transmitted light intensity or the emission intensity was simultaneously observed. Applied field strength was evaluated from the applied voltage divided by the thickness. The field-induced change, measured as a root-mean-square voltage by the lock-in amplifier, was multiplied by $2\sqrt{2}$ to convert it to an equivalent dc voltage. The electroabsorption and electrofluorescence spectra were obtained by plotting the change in absorption intensity and in fluorescence intensity as a function of wavenumber, respectively. Hereafter, electroabsorption and electrofluorescence spectra are abbreviated as E-A and E-F spectra, respectively, and applied electric field is denoted by $\boldsymbol{F}$.

Measurements of the field-induced change in fluorescence decay profile were carried out with a single-photon counting system combined with a homemade pulse generator supplying a bipolar square wave.[49] Output pulses from a mode-locked Ti:sapphire laser (Spectra Physics, Tsunami, repetition rate 80 MHz, pulse duration 80 fs) were doubled and used as an excitation light source. The repetition rate was reduced to 4 MHz with a pulse picker (Conoptics, model 350-160). Fluorescence from the sample was detected by a microchannel-plate photomultiplier (Hamamatsu, R3809U-52). The fluorescence signal was amplified, discriminated, and then led to a time-to-amplitude converter system. Fluorescence decays were obtained with a multichannel pulse height analyzer (SEIKO EG&G, model 7700). Applied voltage was a repetition of rectangular waves of positive, zero, negative, and zero bias in turn. The time duration of each bias was 30 ms, but the first 3 ms was a deadtime to exclude an overshooting effect of applied field just after the change in applied voltage. Four decays were collected, corresponding to positive, zero, negative, and zero sample bias. These decays were stored in each of the different memory segments of the multichannel pulse height analyzer. The instrumental response function had a pulse width of ~60 ps (fwhm).

3. Results and Discussion

3.A. External Electric Field Effects on Absorption of Substituted Diphenylpolyenes. A shift of energy level induced by $\boldsymbol{F}$ is well known as the so-called Stark shift, and the magnitude of this effect is dependent on the electric dipole moment ($\boldsymbol{\mu}$) and the molecular polarizability ($\boldsymbol{\alpha}$) of the system concerned. When the magnitude of $\boldsymbol{\mu}$ or $\boldsymbol{\alpha}$ in the excited electronic state is different from that in the S_0 state, the absorption spectra as well as the emission spectra are shifted since the magnitudes of the level shift in both states are different from each other. For an isotropic and immobilized sample such as a polymer film where chromophores are randomly distributed, the presence of $\boldsymbol{F}$ will broaden an isolated transition due to the change in electric dipole moment following optical absorption, giving rise to the E-A spectrum, the shape of which is the second derivative of the absorption spectrum. If the change in molecular polarizability is significant, the shape of the E-A spectrum is the first derivative of the absorption spectrum. If the transition moment is affected by $\boldsymbol{F}$, the shape of the E-A spectrum is the same as that of the absorption spectrum.

In the present study, solute diphenylpolyenes can be regarded as randomly distributed in a PMMA film. On the assumption that the original isotropic distribution in a PMMA film is maintained in the presence of $\boldsymbol{F}$, the observed E-A spectrum ($\Delta A(\nu)$) may be given by the following equation:[17,18]

$$\Delta A(\nu) = (f\boldsymbol{F})^2\left[A'A(\nu) + B'\nu\frac{\mathrm{d}\{A(\nu)/\nu\}}{\mathrm{d}\nu} + C'\nu\frac{\mathrm{d}^2\{A(\nu)/\nu\}}{\mathrm{d}\nu^2}\right] \tag{1}$$

where f is the internal field factor. The coefficient A' depends on the change in transition dipole moment, and B' and C' are given by the following forms:

$$B' = \frac{\Delta\bar{\alpha}/2 + (\Delta\alpha_m - \Delta\bar{\alpha})(3\cos^2\chi - 1)/10}{hc} \tag{2}$$

$$C' = (\Delta\mu)^2\frac{[5 + (3\cos^2\xi - 1)(3\cos^2\chi - 1)]}{30h^2c^2} \tag{3}$$

where $\Delta\mu$ and $\Delta\alpha$ are the differences in electric dipole moment and molecular polarizability, respectively, between the ground (g) and excited (e) states, i.e., $\Delta\boldsymbol{\mu} = \boldsymbol{\mu}_e - \boldsymbol{\mu}_g$ and $\Delta\boldsymbol{\alpha} = \boldsymbol{\alpha}_e - \boldsymbol{\alpha}_g$:

$$\Delta\mu = |\Delta\boldsymbol{\mu}|; \quad \Delta\bar{\alpha} = (1/3)\mathrm{Tr}(\Delta\boldsymbol{\alpha}) \tag{4}$$

$\Delta\alpha_m$ denotes the diagonal component of $\Delta\boldsymbol{\alpha}$ with respect to the direction of the transition dipole moment; χ is the angle between the direction of $\boldsymbol{F}$ and the electric vector of the excitation light; and ξ is the angle between the direction of $\Delta\boldsymbol{\mu}$ and the transition dipole moment. For the internal field, the Lorentz field correction is used; $f = (\epsilon+2)/3$ with the dielectric constant ϵ of the medium. Under the present experimental conditions, $\chi =$

---

[49] Tsushima, M.; Ushizaka, T.; Ohta, N. *Rev. Sci. Instrum.* **2004**, *75*, 479.

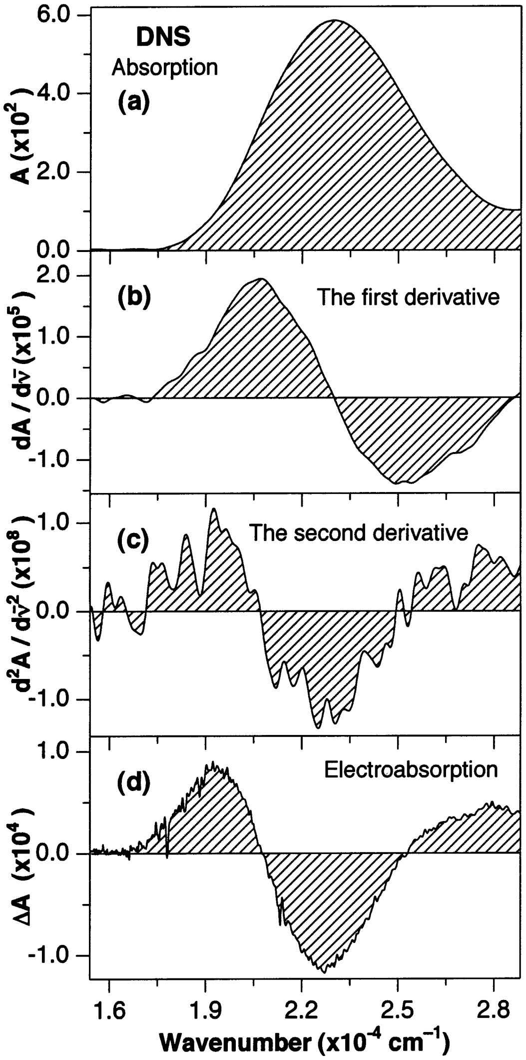

Figure 2. Absorption spectrum, its first and second derivative spectra, and E-A spectrum of DNS at 0.15 mol % in a PMMA film (from top to bottom). Applied field strength was 0.4 MV cm^{-1}.

90° and ϵ of PMMA is 3.6.[50] From eqs 1−4, the values of $\Delta\mu$ and $\Delta\bar{\alpha}$ can be obtained from the analyses of the derivative parts of the E-A spectrum. Solvatochromism of fluorescence can also estimate the magnitude of the dipole moments in fluorescent excited states; however, the analysis of the E-A spectrum has the advantages of estimating the magnitude of the dipole moments in FC states and of eliminating microscopic solute−solvent interactions, which interfere with the estimation of $\Delta\mu$ in solvatochromism measurements.

We have measured the E-A spectra of substituted diphenylpolyenes, to investigate the substitution dependence of the magnitude of $\Delta\boldsymbol{\mu}$ and $\Delta\boldsymbol{\alpha}$ between the FC state and the S$_0$ state. As examples of the E-A spectra of substituted diphenylpolyenes, Figures 2 and 3 show the E-A spectra of DNS and NS at 0.15 mol % in a PMMA film, respectively, together with the absorption spectra and their first and second derivative spectra. The magnitude of the field-induced change in absorption intensity is proportional to the square of applied field strength, as expected from eq 1. In the present study, we focus our attention on the strong absorption, which is assigned to the $\pi\pi^*$ transition to the lowest optically allowed excited state. Equation 1 indicates that the E-A spectrum can be simulated by a linear combination among the absorption spectrum and its first and second derivative spectra. The component of the absorption spectrum is first estimated from the integration of the intensity of the E-A spectrum across the whole spectrum region, since the derivative components do not give a change in total intensity. The residual derivative part is easily divided into the first and second derivative spectra. As shown in Figure 2, the shape of the E-A spectrum of DNS is very similar to that of the second derivative of the absorption spectrum, indicating that the field-induced change in absorption intensity essentially comes from the change in electric dipole moment following the absorption. The E-A spectra of DS, NMS, DCS, and DNB are also essentially the same in shape as the second derivative of the absorption spectrum, while not only the second derivative spectrum but also a small contribution of the first derivative spectrum is necessary to reproduce the E-A spectrum of NS (see Figure 3). The component of the absorption spectrum, i.e., the coefficient A' in eq 1, is negligibly small in all the observed E-A spectra, indicating that the transition dipole moment to the lowest optically allowed excited state is hardly affected by $\boldsymbol{F}$.

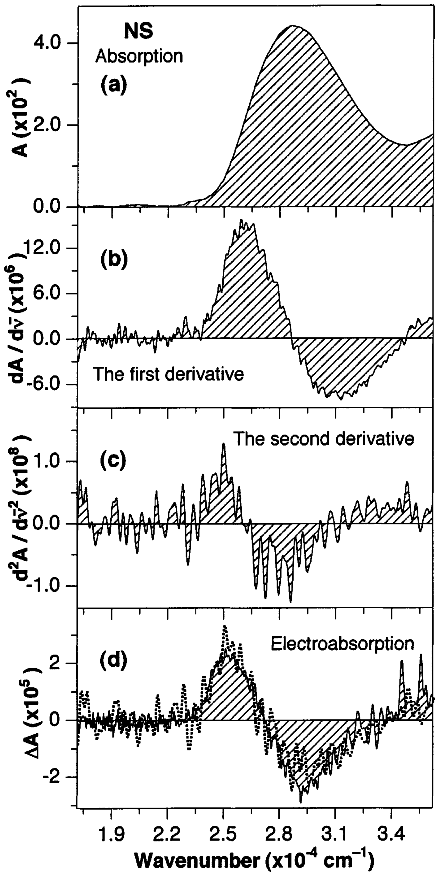

Figure 3. Absorption spectrum, its first and second derivative spectra, and E-A spectrum of NS at 0.15 mol % in a PMMA film (from top to bottom). The simulated E-A spectrum is also shown in (d) by a dotted line. Applied field strength was 0.4 MV cm^{-1}.

The magnitudes of $\Delta\boldsymbol{\mu}$ between the $\pi\pi^*$ FC state and the S$_0$ state in a PMMA film obtained by the analyses of the E-A spectra are shown in Table 1, together with the differences between the Hammet constants of the substituents ($\Delta\sigma$). The angle of ξ is assumed to be 0° in the present study.[31,51] E-A spectra generally do not provide the sign of the change in $\Delta\boldsymbol{\mu}$;

---

(50) *Polymer Handbook*; Brandrup, J., Immergut, E. H., Eds.; John Wiley & Sons: New York, 1975.

Table 1. Magnitude of $\Delta\boldsymbol{\mu}$ between the Franck–Condon Excited State and the Ground State of Substituted Diphenylpolyenes Doped in a PMMA Film

	donor	acceptor	$\Delta\sigma$	$\Delta\mu$ (D)
NS	H	NO_2	−0.78	4.5
DS	$N(Me)_2$	H	−0.83	3.8
NMS	OMe	NO_2	−1.05	7.3
DCS	$N(Me)_2$	CN	−1.49	9.2
DNS	$N(Me)_2$	NO_2	−1.61	10.9
DNB	$N(Me)_2$	NO_2	−1.61	11.6

however, the directions of the dipole moments of donor–acceptor-substituted polyenes are considered to be the same in the S_0 state and in the $\pi\pi^*$ FC state. Since the dipole moments of the substituted stilbenes used are less than 9 D,[24,42] the magnitude of the dipole moment in the $\pi\pi^*$ FC state can be regarded to be larger than in the S_0 state. As shown in Table 1, the magnitude of $\Delta\boldsymbol{\mu}$ becomes larger with the increase of $|\Delta\sigma|$. In the S_0 state, the dipole moment of the substituted stilbene is known to increase in keeping with $|\Delta\sigma|$.[24] Thus the present results indicate that the dipole moment in the $\pi\pi^*$ FC state also becomes larger with increasing $|\Delta\sigma|$. The large enhancement of the dipole moment in the $\pi\pi^*$ FC state suggests that the charge separation between the electron donor and acceptor moieties is enhanced by the excitation to the $\pi\pi^*$ FC state.

The dominance of the second derivative component in the E-A spectrum makes it difficult to estimate the magnitude of $\Delta\boldsymbol{\alpha}$. Only in the E-A spectrum of NS, the first derivative component could be evaluated precisely, since the value of $\Delta\boldsymbol{\mu}$ of NS is not so large. The magnitude of $\Delta\boldsymbol{\alpha}$ of NS is determined to be ~90 Å^3, by assuming that the molecular polarizability is isotropic, i.e., $\Delta\alpha_m = \Delta\bar{\alpha}$.

As already mentioned, DNS and DNB are known to exhibit the ICT process from the LE state to the nonradiative CT state in polar solvents. The LE state may correspond to the $\pi\pi^*$ FC state. In the present study, the magnitude of $\Delta\boldsymbol{\mu}$ of DNS following photoexcitation to the $\pi\pi^*$ FC state in a PMMA film is determined to be 10.9 D. The dipole moment of DNS in the S_0 state is reported to be 7.2–8.2 D.[24,36] Thus, the dipole moment of DNS in the $\pi\pi^*$ FC state can be estimated to be 18.1–19.1 D in a PMMA film. This fairly large dipole moment in the $\pi\pi^*$ FC state suggests that DNS has already exhibited large CT character immediately after the photoexcitation. The present experimental result is in good agreement with the recent theoretical calculation by Farztdinov and Ernsting.[36] With the SAM1/COSMO Hamiltonian, they evaluated the dipole moment of DNS in the FC excited state to be 22 D in the gas phase.

The difference in the magnitude of $\Delta\boldsymbol{\mu}$ between DNS and DNB is as small as 0.7 D (see Table 1), although the conjugated length of DNB is about 2 Å longer than that of DNS. This suggests that a large increase of the charge delocalization occurs in the FC state of DNB, which interferes with the significant enhancement of the dipole moment.

3.B. External Electric Field Effects on Fluorescence of Substituted Diphenylpolyenes. Three stilbenes and one diphenylbutadiene (DS, DCS, DNS, and DNB) exhibit fluorescence that is strong enough for the observation of the electric field effects. Figure 4 shows the E-F spectra of these substituted diphenylpolyenes in a PMMA film, together with the fluorescence spectra simultaneously observed. Note that excitation was done at the wavelength where the field-induced change in absorption intensity is negligibly small. The shape of the fluorescence excitation spectrum is essentially the same as that of the absorption spectrum, indicating that the fluorescence yield is almost independent of the excitation wavelength. The magnitude of the field-induced change in fluorescence intensity is proportional to the square of applied field strength, as in the case of the field-induced change in absorption intensity. In contrast to the E-A spectra, a field-induced quenching of fluorescence is observed and the E-F spectra are reproduced by a superposition of the fluorescence spectrum and its first and second derivative spectra (see Figure 4). The quenching is prominent in the E-F spectra of DNS and DNB. Table 2 shows the magnitude of the field-induced fluorescence quenching of the substituted diphenylpolyenes. In the analysis of the E-F spectrum, we first integrated the intensity of the E-F spectrum across the whole spectrum region to evaluate the magnitude of fluorescence quenching, since the derivative components do not give a change in total intensity. When the fluorescence yield at zero field and its field-induced change are denoted by Φ_F and $\Delta\Phi_F$, respectively, the field-induced change in fluorescence yield relative to the total fluorescence yield is given

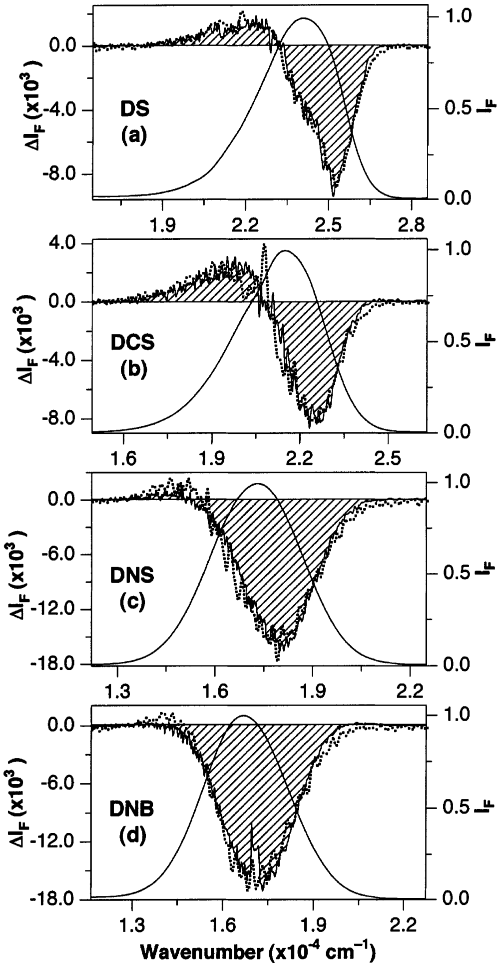

Figure 4. E-F spectra (shaded trace) of DS (a), DCS (b), DNS (c), and DNB (d) in a PMMA film, together with the fluorescence spectra simultaneously observed (solid line). Excitation wavelength was 311.0 nm for DS, 354.0 nm for DCS, 395.5 nm for DNS, and 408.0 nm for DPB. Applied field strength was 0.5 MV cm^{-1} for DS, 0.45 MV cm^{-1} for DCS, and 0.4 MV cm^{-1} for DNS and DNB. The concentration was 0.15 mol % in all the spectra. The simulated E-F spectrum is also shown by a dotted line in every case.

---

(51) Cao, X.; McHale, J. L. *J. Phys. Chem. B* **1997**, *101*, 8843.

Table 2. Quenching of Fluorescence ($\Delta\Phi_F/\Phi_F$), Average Fluorescence Lifetime (τ), and Field-Induced Change in Nonradiative Rate Constant (Δk_{nr}) of Substituted Diphenylpolyenes Doped in a PMMA Film

	$\Delta\Phi_F/\Phi_F$[a,b]	τ (ns)[c]	Δk_{nr} (10^7 s^{-1})[d,e]
DS	−0.003 (0.5)	0.62	1.9
DCS	−0.003 (0.45)	0.77	1.9
DNS	−0.011 (0.4)	1.27	5.5
DNB	−0.012 (0.4)	1.40	5.4

[a] The unit of applied electric field in parentheses is MV cm^{-1}. [b] Uncertainty in $\Delta\Phi_F/\Phi_F$ is ±0.001. [c] Fluorescence decay profile was analyzed by using a triexponential decay function (see captions and text for Figures 5 and 6). [d] Eq 5 is used to estimate the Δk_{nr} value. [e] The Δk_{nr} value is normalized to be in the presence of 1.0 MV cm^{-1} by using its quadratic dependence on applied electric field.

by $\Delta\Phi_F/\Phi_F$. In Table 2, the difference in the magnitude of $\Delta\Phi_F/\Phi_F$ between DS and DCS is small, while the magnitude of $\Delta\Phi_F/\Phi_F$ of DNS is about 4 times larger than that of DCS. This suggests that the magnitude of the quenching is not proportional to that of the energy shift induced by the interaction between the dipole moment in the $\pi\pi^*$ FC state and applied electric field (see Table 1). The magnitude of $\Delta\Phi_F/\Phi_F$ is related to fluorescence lifetime (τ) in the absence of $\boldsymbol{F}$ as well as the field-induced change in nonradiative rate constant (Δk_{nr}) by the following equation:[20]

$$\tau\Delta k_{nr} = \left\{-\frac{\Delta\Phi_F}{\Phi_F}\right\}\Big/\left\{\left(1+\frac{\Delta\Phi_F}{\Phi_F}\right)\right\} \qquad (5)$$

where the field-induced change in radiative rate constant is assumed to be negligibly small. In eq 5, the value of $\Delta\Phi_F/\Phi_F$ becomes directly proportional to fluorescence lifetime, if $|\Delta\Phi_F/\Phi_F|$ is much smaller than unity. By using eq 5 and the fluorescence lifetime obtained in a PMMA film, the value of Δk_{nr} of each chromophore can be estimated, as shown in Table 2. The Δk_{nr} value of DNS is over twice as large as those of DCS and DS, indicating that the difference in the magnitude of $\Delta\Phi_F/\Phi_F$ is not solely due to the difference in fluorescence lifetime.

Since the field-induced change in transition dipole moment to the lowest optically allowed excited state is negligibly small, as shown in Figures 2 and 3, the field-induced quenching of fluorescence suggests that the rates of nonradiative processes from the fluorescent states are accelerated by $\boldsymbol{F}$. The most significant nonradiative process of DS and DCS is known to be the twisting of the double bond, resulting in the *trans* to *cis* isomerization.[38−43] For the fluorescent LE states of DNS and DNB, the ICT process to the nonradiative CT state as well as the isomerization should be considered as the significant nonradiative processes. The yield of the intersystem crossing is negligible in DS and DCS,[38−43] and that in DNS is 0.05 in toluene/benzene[32] and decreases with increasing solvent polarity as mentioned before.[23,28,32] It has been shown that the CT rates are notably affected by $\boldsymbol{F}$ in mixtures of donor and acceptor molecules and methylene-linked molecules of donor and acceptor in a film.[18−20] Thus, the marked field-induced quenching of DNS and DNB observed in the present study can be attributable to the field-induced enhancement of the rate of the ICT process from the fluorescent LE state to the nonradiative CT state.

To quantitatively evaluate the magnitude of the field-induced decrease in lifetime of the LE fluorescence, we have carried out the direct measurements of the field-induced change in fluorescence decay profile for DNS and DNB. Figure 5a shows the fluorescence decay profile of DNS in a PMMA film in the absence of $\boldsymbol{F}$, together with the instrumental response function and the simulated decay. The excitation wavelength was 395.5 nm, where the field-induced change in absorption intensity is negligible (Figure 2). The monitoring wavelength at 560.0 nm is close to the fluorescence maximum; the peak wavelength of the fluorescence of DNS in a PMMA film is 580 nm, which is almost the same as that of the fluorescence in toluene.[28] DNS molecules doped in a PMMA film show a multiexponential fluorescence decay, which probably arises from inhomogeneous environments in a polymer film, i.e., the presence of different interactions between DNS and PMMA which give different fluorescence lifetimes from each other.[52] As shown in Figure 5a, fluorescence decay profiles of DNS could be reproduced by using a triexponential decay, i.e., $\sum_i A_i \exp(t/\tau_i)$, where A_i

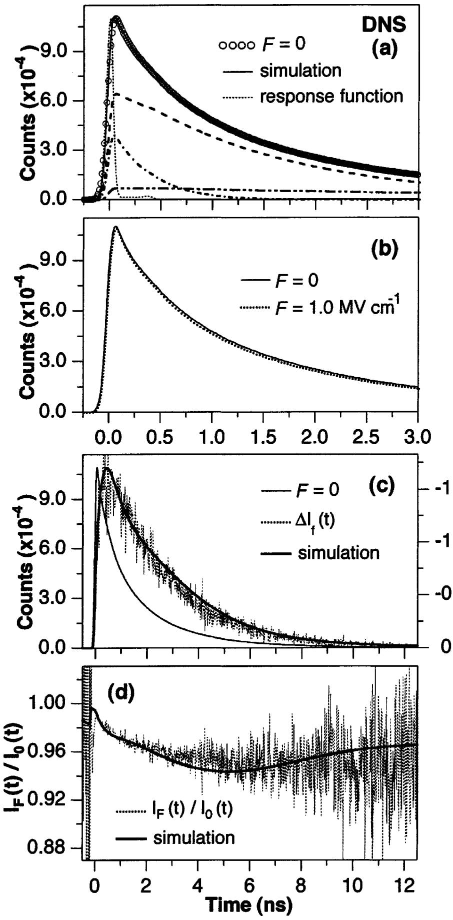

Figure 5. (a) Fluorescence decay (open circles) of DNS at 0.15 mol % in a PMMA film observed at zero field, together with the simulated curve of the decay (solid line) by a convolution of a response function (dotted line) with a triexponential decay. Dashed, dot−dashed, and dot−dot dashed lines represent the decomposed decay components of the simulated decay. Excitation and monitoring wavelengths were 395.5 and 560.0 nm, respectively. (b) Fluorescence decays observed at zero field (solid line) and at 1.0 MV cm^{-1} (dotted line). (c) Difference (dotted line) between the decays observed at 1.0 MV cm^{-1} and at zero field, together with the simulated difference (thick solid line) and the fluorescence decay observed at zero field (thin solid line). (d) Ratio of the decay observed at 1.0 MV cm^{-1} relative to that at zero field (dotted line), together with the simulated one (solid line).

---

(52) Ishikawa, M.; Ye, J. Y.; Maruyama, Y.; Nakatsuka, H. *J. Phys. Chem. A* **1999**, 103, 4319.

Table 3. Time Constants and Pre-exponential Factors of DNS and DNB Doped in a PMMA Film for Different Electric Fields[a,b]

	F (MV cm^{-1})	τ_1 (ns)	τ_2 (ns)	τ_3 (ns)
DNS	0	0.34 (0.388)	1.55 (0.552)	4.64 (0.060)
DNS	1.0	0.31 (0.389)	1.49 (0.550)	4.58 (0.060)
DNB	0	0.47 (0.336)	1.78 (0.645)	4.87 (0.019)
DNB	0.85	0.44 (0.337)	1.73 (0.644)	4.82 (0.019)

[a] Pre-exponential factor of each component is given in parentheses. [b] τ_1 and τ_2 values are subject to an error of up to 0.1%, and τ_3 values are subject to an error of up to 0.2%.

and τ_i denote the pre-exponential factor and lifetime of component i, respectively. The obtained lifetime and the pre-exponential factor of each component are shown in Table 3. The average parameters are considered to be very useful to understand the physical nature of polymer systems in which the inhomogeneous environment is essential. The average lifetime ($\bar{\tau}_f$), defined by $\sum_i A_i\tau_i/\sum_i A_i$, is estimated to be 1.27 ns for DNS at zero field.

Figure 5b shows the fluorescence decays of DNS observed in the absence and in the presence of an electric field of 1.0 MV cm^{-1}, being denoted by $I_0(t)$ and $I_F(t)$, respectively. Both decays obtained at positive bias and at negative bias were essentially the same probably because of a homogeneous distribution of orientations of chromophores in a PMMA film. A small field-induced decrease in fluorescence intensity is observed during the full decay. The difference between the decays observed in the absence and in the presence of $\boldsymbol{F}$, i.e., $I_F(t) - I_0(t)$, referred to as $\Delta I_f(t)$, is shown in Figure 5c. $\Delta I_f(t)$ gives a negative intensity during the full decay. This shows the field-induced quenching of fluorescence. The time dependence of $\Delta I_f(t)$ is apparently different from that of $I_0(t)$, indicating that the fluorescence lifetime is markedly influenced by $\boldsymbol{F}$. If the fluorescence lifetime is independent of $\boldsymbol{F}$, the intensity ratio between two decays observed with and without $\boldsymbol{F}$ should remain constant over the whole time region. As shown in Figure 5d, however, the value of $I_F(t)/I_0(t)$ is not constant during the full decay, but decreases with increasing time. These results indicate that the fluorescence lifetime of DNS is reduced in the presence of $\boldsymbol{F}$. Such a field-induced decrease in fluorescence lifetime can be attributed to the field-induced acceleration of the nonradiative transition from the fluorescent LE state. Both the time profiles of $\Delta I_f(t)$ and $I_F(t)/I_0(t)$ are very sensitive to the parameters of a triexponential decay[49] and are satisfactorily reproduced by using the parameters shown in Table 3. The $\bar{\tau}_f$ value of DNS at 1.0 MV cm^{-1} is then estimated to be 1.21 ns. It is noted in Table 3 that A_i is unaffected by $\boldsymbol{F}$, although τ_i depends on $\boldsymbol{F}$.

Figure 6a shows the fluorescence decay profile of DNB in a PMMA film at zero field. The excitation wavelength was 408.0 nm, where the field-induced change in absorption intensity is negligible, and the monitoring wavelength was 590.0 nm. Note that fluorescence of DNB shows a maximum intensity at 600 nm in a PMMA film. The decay profile of DNB is also reproduced by using a triexponential decay. Figure 6b shows the fluorescence decays of DNB at zero field and in the presence of 0.85 MV cm^{-1}. A field-induced de-enhancement of the fluorescence intensity is observed during the full decay. Figures 6c and 6d show the time profiles of $\Delta I_f(t)$ and $I_F(t)/I_0(t)$ of DNB, respectively. In Figure 6c, $\Delta I_f(t)$ gives a negative intensity during the full decay, and the time dependence of $\Delta I_f(t)$ is different from that of $I_0(t)$. The value of $I_F(t)/I_0(t)$ decreases with increasing time in Figure 6d. These results clearly indicate that the fluorescence lifetime of DNB is also reduced in the presence of $\boldsymbol{F}$. All the observed profiles shown in Figure 6 are well fitted by using a triexponential decay. The lifetime and pre-exponential factor of each component of DNB at zero field and at 0.85 MV cm^{-1} are collected in Table 3. Then, the $\bar{\tau}_f$ value of DNB is estimated to be 1.40 ns at zero field and 1.35 ns at 0.85 MV cm^{-1}.

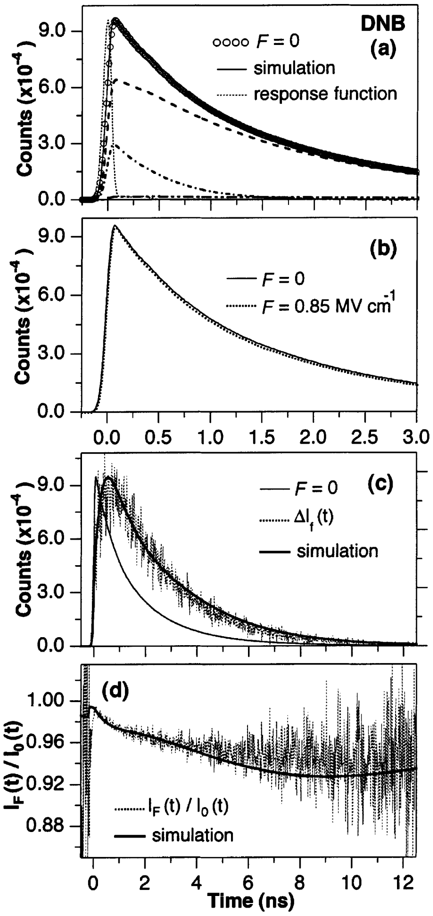

Figure 6. (a) Fluorescence decay (open circles) of DNB at 0.15 mol % in a PMMA film observed at zero field, together with the simulated curve of the decay (solid line) by a convolution of a response function (dotted line) with a triexponential decay. Dashed, dot−dashed, and dot−dot dashed lines represent the decomposed decay components of the simulated decay. Excitation and monitoring wavelengths were 408.0 and 590.0 nm, respectively. (b) Fluorescence decays observed at zero field (solid line) and at 0.85 MV cm^{-1} (dotted line). (c) Difference (dotted line) between the decays observed at 0.85 MV cm^{-1} and at zero field, together with the simulated difference (thick solid line) and the fluorescence decay observed at zero field (thin solid line). (d) Ratio of the decay observed at 0.85 MV cm^{-1} relative to that at zero field (dotted line), together with the simulated one (solid line).

The average value of Δk_{nr} can now be evaluated by subtraction of $1/\bar{\tau}_f$ at zero field from that at $\boldsymbol{F}$; the Δk_{nr} values of DNS and DNB in the presence of 1.0 MV cm^{-1} are determined to be 3.9×10^7 and 3.7×10^7 s^{-1}, respectively. These values are in reasonable agreement with those obtained from the magnitude of $\Delta\Phi_F/\Phi_F$ in Table 2, confirming that the quenching of fluorescence is mainly due to the field-induced decrease in fluorescence lifetime. As shown in Table 3, not only the average fluorescence lifetime but also the lifetime of every decaying component becomes shorter in the presence of $\boldsymbol{F}$. The decaying components exhibit a different efficiency of the field

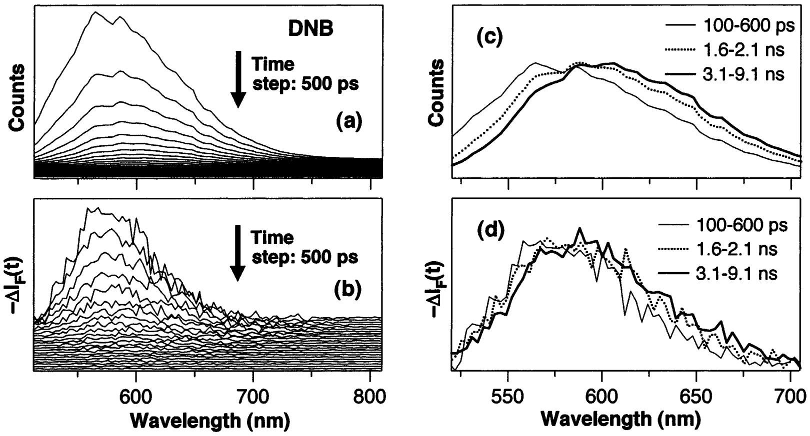

Figure 7. Time-resolved fluorescence spectra (a) and E-F spectra (b) of DNB at 0.15 mol % in a PMMA film. Applied field strength was 0.95 MV cm^{-1}. Excitation wavelength was 408.0 nm. Time interval with which fluorescence intensity was integrated was 500 ps. Time-resolved fluorescence spectra and E-F spectra of DNB, where the peak intensities are normalized to unity, are shown in (c) and (d), respectively. Fluorescence spectra in (c) and (d) were measured with a time interval of 100−600 ps (thin solid line), 1.6−2.1 ns (dotted line), and 3.1−9.1 ns (thick solid line).

dependence. In both DNS and DNB, the fastest decaying component shows the most efficient decrease in lifetime by $\boldsymbol{F}$; the lifetime of the fastest decaying component of DNS becomes shorter by a factor of 9% at 1.0 MV cm^{-1}.

The measurements of the time-resolved E-F spectra of DNB in a PMMA film were also carried out with a field strength of 0.95 MV cm^{-1}. Figures 7a and 7b show the time-resolved fluorescence spectra and time-resolved E-F spectra of DNB in a PMMA film, respectively. The time interval with which fluorescence was collected was 500 ps. In Figure 7a, the fluorescence spectrum slightly shifts to a longer wavelength with time. This may come from the presence of different interactions between DNB and PMMA which give different spectral shapes and different fluorescence lifetimes. The time-resolved fluorescence and E-F spectra, where the peak intensities are normalized to unity, are shown in Figures 7c and 7d, respectively. The E-F spectrum in Figure 7d also exhibits a red-shift as a passage of time, but the magnitude of the shift is smaller than that observed in the fluorescence spectrum in Figure 7c. This result suggests that the magnitude of the field-induced quenching of DNB depends on the interaction between DNB and PMMA. The time dependence of the Stark effect line shape should also be considered.

We summarize the results of DNS and DNB obtained using electric field modulation spectroscopy as follows. (1) The fluorescence yields of DNS and DNB are markedly de-enhanced by $\boldsymbol{F}$. (2) $|\Delta\Phi_F/\Phi_F|$ of these molecules are about 4 times larger than those of the other diphenylpolyenes used in the present study. (3) The fluorescence lifetimes of DNS and DNB are reduced in the presence of $\boldsymbol{F}$. (4) The transition moments between the S_0 state and the lowest optically allowed excited state are independent of $\boldsymbol{F}$. As mentioned before, the fluorescence yields of DNS and DNB drastically decrease in polar solvents, which has been attributed to the presence of the transition from the fluorescent LE state to the nonradiative CT state in polar environment.[27−37] From these results, it is now concluded that the ICT rates of DNS and DNB are accelerated by $\boldsymbol{F}$. The ICT processes of DNS and DNB are shown to be controlled by $\boldsymbol{F}$ in the present study.

The energy level of the CT state can be considered to be significantly affected by $\boldsymbol{F}$ because of its large electric dipole moment. This causes a large shift of the free energy gap between the LE and CT states in the presence of $\boldsymbol{F}$. Thus, the ICT dynamics is expected to be affected by $\boldsymbol{F}$, depending on the magnitude of the dipole moment of the CT state. The field-induced increase in ICT rate in a random distribution system is qualitatively explained as follows.[18] The free energy gap of the reaction (ΔG) in the presence of $\boldsymbol{F}$ can be given as $\Delta G_0 - \boldsymbol{\mu F}$, where ΔG_0 is the free energy gap in the absence of $\boldsymbol{F}$ and $\boldsymbol{\mu}$ is the electric dipole moment of the product. The external electric field can be regarded as a perturbation, and thus the CT rate constant is expanded as a power series of $\boldsymbol{F}$. By assuming that only ΔG is affected by $\boldsymbol{F}$ and the CT rate is given by the classical theory, Δk_{CT}, which is defined as $k_{CT}(\boldsymbol{F}) - k_{CT}(\boldsymbol{F} = 0)$, divided by $k_{CT}(\boldsymbol{F} = 0)$ is given by[18]

$$\Delta k_{CT}/k_{CT}(\boldsymbol{F}=0) = 2B(\Delta G_0 + \lambda_0)(\boldsymbol{\mu F}) + B\{2B(\Delta G_0 + \lambda_0)^2 - 1\}(\boldsymbol{\mu F})^2 \quad (6)$$

where B is $(4k_BT\lambda_0)^{-1}$ and λ_0 is the reorganization energy. In eq 6, the zeroth-, the first-, and the second-order terms in $\boldsymbol{F}$ are considered, and other higher terms are neglected. In a random distribution system, the average of $\boldsymbol{\mu F}$ and $(\boldsymbol{\mu F})^2$ integrated over the full space is given by zero and $|\boldsymbol{\mu}|^2|\boldsymbol{F}|^2/3$, respectively. Thus, eq 6 can be rewritten as follows:

$$\Delta k_{CT}/k_{CT}(\boldsymbol{F}=0) = \frac{B}{3}\{2B(\Delta G_0 + \lambda_0)^2 - 1\}|\boldsymbol{\mu}|^2|\boldsymbol{F}|^2 \quad (7)$$

From eq 7, the negative value of Δk_{CT} in a random distribution system is predicted only for a small barrier reaction where the activation energy is smaller than the thermal energy, k_BT. The ICT processes of DNS and DNB occur in the subnano- to nanosecond time range, suggesting that their barrier heights are larger than k_BT. Therefore, the positive value of Δk_{CT} is expected for DNS and DNB, which is consistent with the present experimental results. Recently, Tachiya et al. have proposed detailed theoretical models for field-induced changes in electron transfer.[53] Farztdinov and Ernsting have suggested that all single-bond twisted conformations of DNS in excited states show no emission because of their very small oscillator strengths, and the nitrophenyl- and dimethylamino-twisted conformations are 1 eV below the FC state in polar solvents.[36] Hence, the ICT

---

(53) Hilczer, M.; Tachiya, M. *J. Chem. Phys.* **2002**, *117*, 1759.

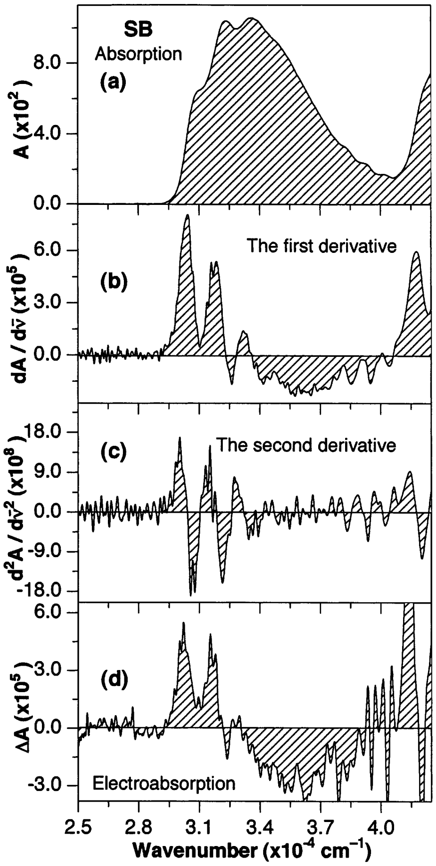

Figure 8. Absorption spectrum, its first and second derivative spectra, and E-A spectrum of SB at 0.5 mol % in a PMMA film (from top to bottom). Applied field strength was 0.75 MV cm^{-1}.

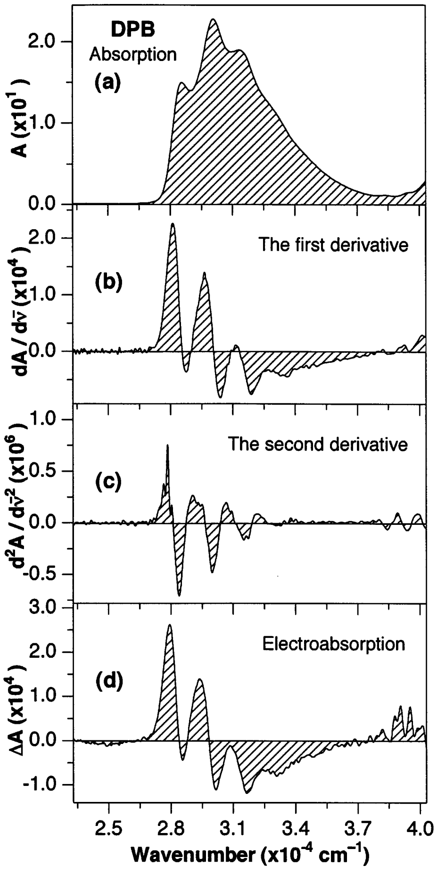

Figure 9. Absorption spectrum, its first and second derivative spectra, and E-A spectrum of DPB at 0.5 mol % in a PMMA film (from top to bottom). Applied field strength was 0.75 MV cm^{-1}.

dynamics from the LE state to the nonradiative CT state of DNS and DNB may be accompanied by geometrical relaxation to the twisted conformations.

3.C. External Electric Field Effects on Absorption and Fluorescence of Unsubstituted Diphenylpolyenes. Figure 8 shows the E-A spectrum of SB at 0.5 mol % in a PMMA film, together with the absorption spectrum and its derivative spectra. The absorption bands observed around 34 000 cm^{-1} are assigned to the $S_1 \leftarrow S_0$ transition, and the vibronic structure arises mainly from the olefinic stretching modes.[54] In contrast to the substituted diphenylpolyenes, the E-A spectrum of SB is similar in shape to the first derivative of the absorption spectrum, as reported in our preliminary paper,[21] indicating that the field-induced change in absorption intensity mainly comes from the change in molecular polarizability following the photoexcitation. Owing to the C_{2h} symmetry, SB molecules in an isolated condition have no permanent electric dipole moment, and it is understood that $\Delta\mu$ is negligible at a low concentration of SB in a film. The field-induced change in total absorption intensity is small, indicating that the transition dipole moment to the S_1 state is hardly affected by $\boldsymbol{F}$.

Figure 9 shows the E-A spectrum of DPB doped in a PMMA film, together with the absorption spectrum and its derivative spectra. The absorption band is assigned to the transition to the S_1 state. The E-A spectrum is very similar in shape to the first derivative of the absorption spectrum, and the field-induced change in total absorption intensity is negligibly small. Thus, the field effects on the absorption spectrum of DPB are essentially the same as the ones observed for SB. The same features are also observed in the E-A spectrum of DPH.

Figure 10 shows the E-F spectra of SB, DPB, and DPH doped in a PMMA film, together with the fluorescence spectra simultaneously observed. These fluorescence spectra are due to the $S_1 \rightarrow S_0$ transition. Note that excitation was done at the wavelength where the field-induced change in absorption intensity is negligible. All the molecules exhibit a decrease in fluorescence intensity in the presence of $\boldsymbol{F}$. The negative components of the E-F spectra indicate that the fluorescence quantum yields of the unsubstituted diphenylpolyenes are reduced by $\boldsymbol{F}$. The E-F spectra of SB and DPB are satisfactorily reproduced by a linear combination of the fluorescence spectrum and its first derivative spectrum (see Figures 10a and 10b). As shown in Figure 10c, however, the E-F spectrum of DPH in a high-wavenumber region cannot be fitted well by a linear combination between the fluorescence spectrum and its first derivative spectrum. This disagreement suggests that the fluorescence of DPH is originated simultaneously from different states. The fluorescence of DPH is known to arise from the 2^1A_g (S_1) state coupled with the optically allowed 1^1B_u (S_2) state;[55-57] however the fluorescence from the 1^1B_u state is slightly observed in the higher-wavenumber side of the 2^1A_g

---

(54) Nakabayashi, T.; Okamoto, H.; Tasumi, M. *J. Phys. Chem. A* **1998**, *102*, 9686.

(55) Saltiel, J.; Ko, D.-H.; Fleming, S. A. *J. Am. Chem. Soc.* **1994**, *116*, 4099.

(56) Itoh, T.; Kohler, B. E. *J. Phys. Chem.* **1987**, *91*, 1760.

(57) Saltiel, J.; Sears, D. F., Jr.; Sun, Y.-P.; Choi, J.-O. *J. Am. Chem. Soc.* **1992**, *114*, 3607.

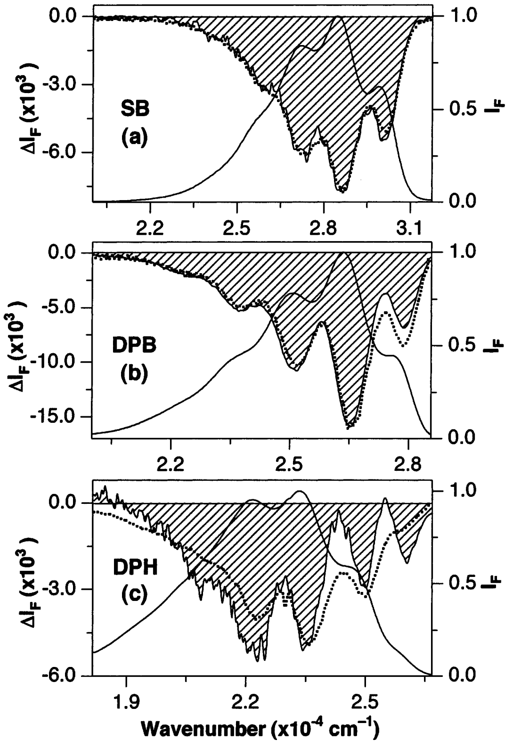

Figure 10. E-F spectra (shaded line) of SB (a), DPB (b), and DPH (c) in a PMMA film, together with the fluorescence spectra simultaneously observed (solid line). Excitation wavelength was 298.5 nm for SB, 335.0 nm for DPB, and 347.0 nm for DPH. Applied field strength was 1.0 MV cm^{-1} for SB and DPB and 0.8 MV cm^{-1} for DPH. The concentration was 0.5 mol % in all the spectra. The simulated E-F spectrum is also shown by a dotted line in every case.

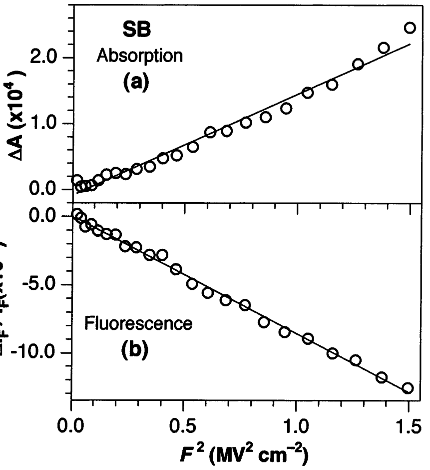

Figure 11. Plots of the field-induced change in absorption intensity (a) and in fluorescence intensity (b) of SB at 0.5 mol % in a PMMA film as a function of the square of applied field strength. The observed absorption and fluorescence wavelengths were 331 and 350 nm, respectively.

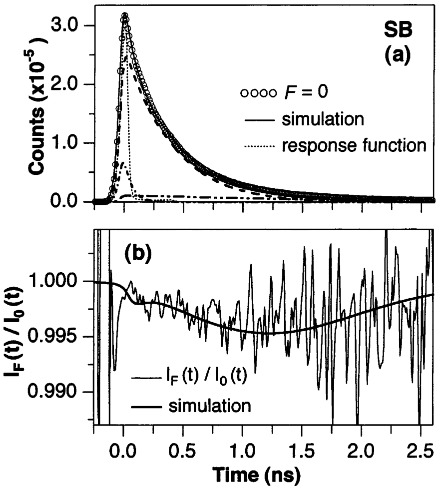

Figure 12. (a) Fluorescence decay (open circles) of SB at 0.5 mol % in a PMMA film, together with the simulated curve of the decay (solid line) by a convolution of a response function (dotted line) with a triexponential decay. Dashed, dot−dashed, and dot−dot dashed lines represent the decomposed decay components of the simulated decay. Excitation and monitoring wavelengths were 298.5 and 350.0 nm, respectively. (b) Ratio of the decay observed at 1.0 MV cm^{-1} relative to that at zero field (thin solid line), together with the simulated one (thick solid line).

fluorescence.[56] The weak fluorescence from the *cis*-conformer is also observed with a peak located at a lower wavenumber than that of the *trans*-conformer.[57] The disagreement between the E-F spectrum and the simulated spectrum for DPH in the high-wavenumber region may be interpreted in terms of the presence of the weak fluorescence from the 1^1B_u state in the high-wavenumber side of the 2^1A_g fluorescence. The magnitude of $\Delta\Phi_F/\Phi_F$ is estimated to be 1.1% for SB at 1.0 MV cm^{-1}, 1.6% for DPB at 1.0 MV cm^{-1}, and 0.5% for DPH at 0.8 MV cm^{-1}. Note that the magnitude of the field-induced change is proportional to the square of applied field strength. Plots of the field-induced change in fluorescence intensity and in absorption intensity of SB against the square of field strength are shown in Figure 11.

The transition moments of the unsubstituted diphenylpolyenes between the S_0 and S_1 states are found to be unaffected by $\boldsymbol{F}$. In all the E-F spectra, the intensity decrease is observed in the whole spectrum region, indicating that the change in the fluorescence intensity is mainly due to the all-*trans*-molecules in the S_1 state. Thus the field-induced fluorescence quenching of the unsubstituted diphenylpolyenes can be ascribed to the field-induced enhancement of the rates of nonradiative processes from the S_1 state. As mentioned below, the measurements of the field-induced change in decay profile of SB also indicate the increase in nonradiative rate constant in the presence of $\boldsymbol{F}$. The fluorescence decay of SB doped in a PMMA film in the absence of $\boldsymbol{F}$ is shown in Figure 12a. The decay profile of SB is well fitted by using a triexponential decay. The time constant and pre-exponential factor of each component at zero field are determined to be as follows: $\tau_1 = 60$ ps, $\tau_2 = 360$ ps, $\tau_3 =$ 1.67 ns and $A_1 = 0.305$, $A_2 = 0.667$, $A_3 = 0.028$. The $\bar{\tau}_f$ value of SB in a PMMA film is then determined to be 305 ps at zero field. The time profile of $I_F(t)/I_0(t)$ of SB is shown in Figure 12b. The shape of $I_F(t)/I_0(t)$ is sensitive to the change in fluorescence lifetime, as shown in Figures 5 and 6. If the fluorescence lifetime is independent of $\boldsymbol{F}$, the intensity ratio should remain constant over the whole time region. As shown in Figure 12b, however, the value of $I_F(t)/I_0(t)$ decreases with increasing time, indicating that the fluorescence lifetime of SB is reduced in the presence of $\boldsymbol{F}$. This result indicates the field-induced acceleration of the nonradiative rates in the S_1 state. The time constant of each component at 1.0 MV cm^{-1} is qualitatively estimated to be as follows: $\tau_1 = 59$ ps, $\tau_2 = 359$ ps, $\tau_3 = 1.67$ ns. The time profile of $I_F(t)/I_0(t)$ is sensitive to the change in τ_i of 0.1%. The magnitude of A_i remains unchanged within the present experimental accuracy.

For SB and DPB in the S_1 state, the *trans* to *cis* isomerization has been known to be one of the significant nonradiative

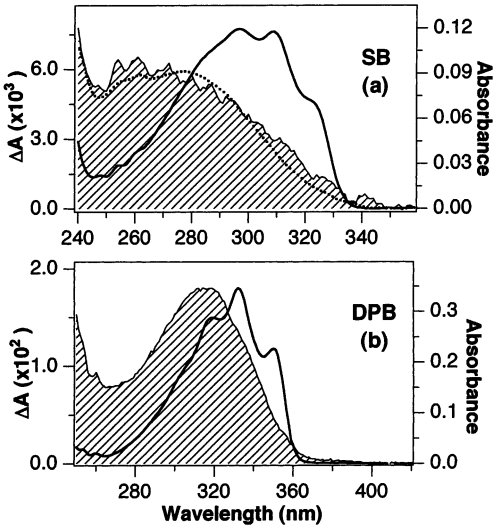

Figure 13. (a) Difference spectrum (shaded line) of SB in a PMMA film obtained by subtraction of the spectrum observed before UV irradiation from that after irradiation with UV light at 298.5 nm, together with the absorption spectrum before the UV irradiation (solid line) and the absorption spectrum of *cis*-stilbene doped in a PMMA film (dotted line). The concentration of SB was 0.5 mol %. (b) Difference spectrum (shaded line) of DPB in a PMMA film obtained by subtraction of the spectrum observed before UV irradiation from that after irradiation with UV light at 335.0 nm, together with the absorption spectrum before the UV irradiation (solid line). The concentration was 0.5 mol %.

pathways.[6−11,58] Actually, the quantum yield of the conversion from the FC state to the *perpendicular* intermediate state of the isomerization is close to unity for SB[8,9,45,46] and is ∼0.22 for DPB[58] in solution. The isomerization yield of DPH has been found not to be so large as that of SB, although this yield is strongly dependent on solvent polarity.[55] It is hence conceivable that the rate of the *trans* to *cis* isomerization increases in the presence of $\boldsymbol{F}$, which results in the field-induced decrease in fluorescence lifetime. To examine whether the *trans* to *cis* photoisomerization occurs or not in a PMMA film, we have compared the absorption spectra of the unsubstituted diphenylpolyenes in a PMMA film obtained before and after UV irradiation.

Figure 13a shows the difference spectrum of SB in a PMMA film obtained by subtraction of the spectrum observed before UV irradiation from that observed after irradiation with UV light at 298.5 nm. A factor that ensured that the vibrational structure of the original absorption spectrum did not remain in the subtracted spectrum was multiplied to the absorption spectrum after the irradiation. The feature of the obtained difference spectrum is similar to that of the absorption spectrum of *cis*-stilbene.[59] Since there is a large potential barrier separating the *trans* and *cis* isomers in the S_0 state, the two isomers are not interchangeable with each other in the S_0 state at room temperature. Hence the difference spectrum in Figure 13a can be attributable to the *cis* isomer generated via the S_1 state of SB. The quantum yield of the *trans* to *cis* photoisomerization can be determined in principle by using the number of doped molecules in the irradiated volume, that of the molecules absorbing photons, and the magnitude of the absorption change. We have qualitatively estimated the isomerization yield to be 0.3 ± 0.15 in a PMMA film at room temperature from the excitation energy of 5.0×10^{-4} J, the spot area of 3.6×10^{-1} cm², and the literature values of the absorption coefficients of the *trans* isomer of $10^{4.49}$ at 307 nm and $10^{4.46}$ at 295 nm. Figure 13b shows the difference spectrum of DPB in a PMMA film by using UV light at 335.0 nm. The difference spectrum of DPB exhibits a peak at ∼314 nm, which is similar to the peak position of the reported absorption spectrum of the *cis*−*trans* form of DPB in hexane solution.[58] These results clearly indicate that the photoexcited all-*trans*-diphenylpolyenes can isomerize to the *cis* configurations even in a PMMA film at room temperature.

In Figure 12a, the fluorescence decay of SB doped in a PMMA film is composed of picosecond and nanosecond decay components. The radiative lifetime of SB is reported to be 1.7−2.7 ns,[60,61] indicating that the picosecond decay component is mainly ascribed to the nonradiative process. This nonradiative process can be regarded as the isomerization to the *cis* configuration (Figure 13a). On the other hand, the nonradiative process is considered to make a small contribution to the nanosecond decay component. From these considerations, it may be concluded that two types of SB exist in a PMMA film: one can easily isomerize to the *cis* configuration via the S_1 state and the other cannot within the radiative lifetime. There are many sizes of free spaces in a PMMA film, so that the former one is assigned to SB molecules existing in large free spaces and the latter one is assigned to those existing in free spaces that are too small for the isomerization. The yield of the photoisomerization to the intermediate state is estimated by the lifetime distribution. On the assumption that the nanosecond decay does not involve the isomerization, the yield to the intermediate state is qualitatively evaluated to be 0.8 in a PMMA film. It has been proposed that the photoisomerization of stilbene does not occur in a PMMA film, since a lifetime of 1.6 ns was observed in SB molecules doped in a PMMA film by transient absorption spectroscopy.[62] However, the present experimental results indicate that SB molecules in large free spaces in a PMMA film can perform the *cis*−*trans* photoisomerization at room temperature. The lifetime of several nanoseconds observed in a film may be ascribed to SB molecules in small free spaces.

From the present absorption and fluorescence experiments, it is now concluded that the isomerization is one of the significant nonradiative pathways for SB and DPB in the S_1 state in a PMMA film. The field-induced quenching of fluorescence as well as the field-induced decrease in fluorescence lifetime can be therefore ascribed to the field-induced enhancement of the rate of the isomerization to the *cis* configurations. As mentioned above, DCS shows the photoisomerization with the large quantum yield in solution: the isomerization yield of DCS is 0.50 in benzene,[38] while that of DNS is 0.02 in the same solvent.[28] The twisting of the C═C bond is also known to be the most efficient nonradiative pathway for DS in the S_1 state.[42,43] Hence it may be said that the quenching components of DCS and DS in Table 2 are mainly due to the field-induced enhancement of the isomerization rate.

The mechanism of the photoisomerization of SB in solution has been proposed as follows.[7−11,45,46,63] The photoexcitation

---

(58) Yee, W. A.; Hug, S. J.; Kliger, D. S. *J. Am. Chem. Soc.* **1988**, *110*, 2164.
(59) Myers, A. B.; Mathies, R. A. *J. Chem. Phys.* **1984**, *81*, 1552.
(60) Sumitani, M.; Nakashima, N.; Yoshihara, K.; Nagakura, S. *Chem. Phys. Lett.* **1977**, *51*, 183.
(61) Saltiel, J.; Waller, A. S.; Sears, D. F., Jr.; Garrett, C. Z. *J. Phys. Chem.* **1993**, *97*, 2516.
(62) Nikowa, L.; Schwarzer, D.; Troe, J.; Schroeder, J. *J. Chem. Phys.* **1992**, *97*, 4827.
(63) Hochstrasser, R. M. *Pure Appl. Chem.* **1981**, *52*, 2683.

of SB with UV light results in a *trans* S_1 species having a planar structure. On the S_1 potential surface, the generated S_1 species is thermally activated to go over the barrier in a picosecond time scale to form another S_1 species with a 90° twisted structure around the C=C bond. This *perpendicular* species then relaxes very rapidly (<1 ps) to a *perpendicular* S_0 species, which transforms to the *trans* and *cis* isomers with nearly the same ratio. In this scheme, it is noted that the barrier in the photoisomerization only occurs between the *trans* and *perpendicular* structures on the S_1 potential surface. Thus, the rate-limiting step in the overall *trans* to *cis* photoisomerization is the barrier crossing to the *perpendicular* configuration in the S_1 state.

From the solvent dependence of the optical spectra of SB and tetraphenylethylene, it has been suggested that the *perpendicular* intermediate state on the S_1 potential surface is likely to be a zwitterionic state with a large dipole moment.[64−67] The zwitterionic intermediate is also proposed in the photoisomerization of DPH for the terminal bond.[55] Recently, Amatatsu has estimated the electronic structure of SB at the conical intersection by complete-active-space self-consistent-field (CASSCF) calculations.[68] The conical intersection was calculated to be a crossing region between a zwitterionic state and a covalent state in S_0 and S_1. If the *perpendicular* intermediate state in the S_1 state has zwitterionic or charge transfer character, the activated barrier crossing from the *trans* configuration to the intermediate state on the S_1 potential surface can be regarded as the ICT process. In such a case, the photoisomerization may be affected by $\boldsymbol{F}$ as discussed in subsection 3.B. In the present study, fluorescence yields of the unsubstituted all-*trans*-diphenylpolyenes are reduced by $\boldsymbol{F}$, suggesting the field-induced enhancement of the photoisomerization to the *cis* configurations. Therefore, the present result may suggest the zwitterionic model at the intermediate state of the *trans* to *cis* photoisomerization in a PMMA film.

4. Conclusions

In the present study, we have measured the E-A and E-F spectra of *para*-substituted and unsubstituted all-*trans*-diphenylpolyenes doped in a PMMA film. The E-A spectra of the substituted diphenylpolyenes are essentially the same in shape as the second derivative of the absorption spectrum, indicating that the field-induced change in absorption intensity mainly comes from the change in electric dipole moment following absorption. The analysis of the E-A spectra indicates that the dipole moment of the substituted stilbene in the $\pi\pi^*$ FC state becomes larger with the increase of the magnitude of $\Delta\sigma$. The large enhancement of the dipole moment in the $\pi\pi^*$ FC state suggests that the charge separation between the electron donor and acceptor substituents is enhanced in the $\pi\pi^*$ FC state.

Fluorescence yields of DNS and DNB are markedly reduced by $\boldsymbol{F}$, indicating that the ICT rates from the fluorescent LE state to the nonradiative CT state of DNS and DNB are accelerated by $\boldsymbol{F}$. The direct measurements of the field-induced change in fluorescence lifetime are carried out for DNS and DNB with a picosecond time resolution. The average lifetime of the fluorescent LE state of DNS is 1.27 ns at zero field and 1.21 ns at 1.0 MV cm^{-1}, and that of the fluorescent LE state of DNB is 1.40 ns at zero field and 1.35 ns at 0.85 MV cm^{-1}. The ICT processes of DNS and DNB are shown to be controlled by $\boldsymbol{F}$. It is noted that the magnitude of $\Delta\boldsymbol{\mu}$ between the $\pi\pi^*$ FC state and the S_0 state of DNS is estimated to be 10.9 D, indicating that DNS exhibits large CT character immediately after photoexcitation.

We have shown that the *trans* to *cis* isomerization is a significant nonradiative process for SB and DPB doped in a PMMA film. This photoisomerization is found to be accelerated by $\boldsymbol{F}$, suggesting that the intermediate state of the photoisomerization in the S_1 state has zwitterionic or charge transfer character. Analyses of the field effects on the photoexcitation dynamics with the recent theoretical model[67] will give detailed information on the electronic structure around the conical intersection. In some biological systems, charged and polar groups of the protein surrounding chromophores produce strong electric fields. The present result suggests that electric fields generated from the protein significantly influence photochemical reactions of chromophores in protein environment.

Measurements of solvent polarity dependence of optical spectra are generally used to obtain information on CT processes or CT characters in the systems. This method is useful; however, microscopic solute−solvent interactions as well as dependencies of the spectra on other solvent parameters often interfere with the estimation of the CT characters. Since an external electric field is the only perturbation to be considered, measurements of external electric field effects on optical spectra are expected to provide detailed information on photoisomerization as well as CT dynamics.

Acknowledgment. This work has been supported in part by Grants-in-Aid for Scientific Research (Grant Nos. 15205001, 15655001, and 15685005) and for Scientific Research on Priority Area (417) from the Ministry of Education, Culture, Sports, Science, and Technology in Japan.

JA0401444

---

(64) Hicks, J. M.; Vandersall, M. T.; Sitzmann, E. V.; Eisenthal, K. B. *Chem. Phys. Lett.* **1987**, *135*, 413.
(65) Schilling, C. L.; Hilinski, E. F. *J. Am. Chem. Soc.* **1988**, *110*, 2296.
(66) Rodier, J.-M.; Myers, A. B. *J. Am. Chem. Soc.* **1993**, *115*, 10791.
(67) Deckert, V.; Iwata, K.; Hamaguchi, H. *J. Photochem. Photobiol. A: Chem.* **1996**, *102*, 35.
(68) Amatatsu, Y. *Chem. Phys. Lett.* **1999**, *314*, 364.